

# Colorimetric immunodetection of bacteria enriched on membranes within a compact multichannel filtration device

## Journal Article

### Author(s):

Tang, Jiukai; Meng, Yingchao ; Bezinge, Léonard ; Qiu, Guangyu ; Yue, Yang; Zhang, Xiaole; Wang, Jing

### Publication date:

2022-02-15

### Permanent link:

<https://doi.org/10.3929/ethz-b-000518864>

### Rights / license:

[Creative Commons Attribution 4.0 International](#)

### Originally published in:

Sensors and Actuators B: Chemical 353, <https://doi.org/10.1016/j.snb.2021.131142>



## Colorimetric immunodetection of bacteria enriched on membranes within a compact multichannel filtration device

Jiukai Tang<sup>a,b</sup>, Yingchao Meng<sup>c</sup>, Léonard Bezinge<sup>c</sup>, Guangyu Qiu<sup>a,b</sup>, Yang Yue<sup>a,b</sup>, Xiaole Zhang<sup>a,b</sup>, Jing Wang<sup>a,b,\*</sup>

<sup>a</sup> Institute of Environmental Engineering, ETH Zürich, Zürich 8093, Switzerland

<sup>b</sup> Laboratory for Advanced Analytical Technologies, Empa, Swiss Federal Laboratories for Materials Science and Technology, Dübendorf 8600, Switzerland

<sup>c</sup> Institute of Chemical and Bioengineering, ETH Zürich, Zürich 8093, Switzerland

### ARTICLE INFO

#### Keywords:

Colorimetric immunodetection  
Membrane filter  
Bacteria enrichment  
Multichannel filtration  
Smartphone

### ABSTRACT

Colorimetric immunoassay is a widely used method for pathogen detection. The conventional implementation of immunoassays in 96-well plates often encounters difficulties for samples with low concentrations. In this study, the detection performance has been improved using a cellulose acetate membrane for target enrichment and immunodetection. For this end, a compact multichannel filtration device was fabricated using a 3D printer for sample loading. Background effects of the membrane were greatly minimized after pretreatment with a sodium hydroxide solution to significantly reduce non-specific binding. The colorimetric result of the immunodetection of *Escherichia coli* strain K12 (*E. coli* K12) was recorded and quantitatively analyzed with a smartphone camera. A limit of detection was calculated as 40 cfu (colony forming unit)/ml, two orders of magnitude more sensitive than that obtained on 96-well plates with standard protocol. The developed approach features an integrated sample enrichment scheme, reduced reagents consumption, multiple channels for parallel processing and no reliance on advanced laboratory instruments, thereby providing potential for a low-cost and easy-to-use immunodetection system.

### 1. Introduction

Pathogen detection is an important aspect of biosafety assessment in the fields of water supply [1–3], air quality management [4–6] and food storage [7–10]. Currently, main methods for pathogen detection include the culture-based methods, the molecular methods and the immunoassays [11,12]. Culture-based method is intuitive and requires almost no analysis instruments. That said, only part of the pathogens can actually be cultured, which might lead to underestimated results [13,14]. Additionally, the culture process is time-consuming and accurate species information is difficult to be gathered merely from the colonies. As a typical molecular method for pathogen detection, the polymerase chain reaction (PCR) method significantly improves the analysis sensitivity and specificity. However, the complexity resulted from sample preparation, strict requirement of temperature control and high dependence on advanced instruments make the PCR method challenging to operate and unsuitable for low cost applications [15]. In contrast, immunoassays relying on the specific interaction between the antigen and antibody,

present multiple advantages including less-intensive efforts, fast response and good specificity [16]. Additionally, the colorimetric visualization of immunodetection results enables the development of portable and low-cost devices [7,10]. Conventionally, the colorimetric immunodetection of pathogens can be carried out in 96-well plates according to commercial protocols. However, it is not recommended for detecting samples with concentrations lower than  $10^4$  -  $10^5$  cfu/ml [8]. Although preconcentration methods can be used to improve the sensitivity in 96-well plates, this additional step increases the complexity of the assay and may lead to the loss of analytes during sample transfer. Therefore, it is of significance to integrate the sample enrichment and colorimetric immunodetection on the same substrate for simplifying the analysis process and improving the detection performance.

Membranes are commonly used for sample purification and concentration. In recent years, membranes have also been selected as novel substrates for immunodetection. One typical application is the nitrocellulose membrane based lateral flow immunoassay [15,17]. It provides visual detection of pathogens with fast responses and simple

\* Corresponding author at: Institute of Environmental Engineering, ETH Zürich, Zürich 8093, Switzerland.

E-mail address: [jing.wang@ifu.baug.ethz.ch](mailto:jing.wang@ifu.baug.ethz.ch) (J. Wang).

<https://doi.org/10.1016/j.snb.2021.131142>

Received 23 August 2021; Received in revised form 19 October 2021; Accepted 21 November 2021

Available online 25 November 2021

0925-4005/© 2021 The Author(s). Published by Elsevier B.V. This is an open access article under the CC BY license (<http://creativecommons.org/licenses/by/4.0/>).

operations. Nevertheless, as the lateral flow based device cannot work efficiently for sample enrichment, it has a limited advantage in detecting low concentration of pathogens and has been mostly employed for qualitative or semiquantitative applications [18]. For example, the detectable concentration of *E.coli O157:H7* using lateral flow immunoassays was usually higher than  $10^4$ - $10^5$  cfu/ml [19,20]. In contrast, as another membrane based application, the vertical flow immunoassay shows overwhelming advantage in combining sample purification and enrichment [21–24].

Commercial membranes usually have large areas with diameters in the range of ten to hundred millimeters. For immunodetection, these large membranes require high volume of antibody reagents. For instance, Ezenarro et al. applied the membranes with a 25 mm diameter as the immunodetection substrate [22]. Consequently, 0.5 ml antibody reagent had to be consumed for each sample. Besides high reagent consumption, dispersion of analyte on large membranes could lead to an insensitive color development. To address these problems, we have developed a compact filtration system combining miniaturized membranes within a 3D-printed device. The device incorporates multiple channels to enhance analysis throughput and contributes to the development of portable devices.

In this proof-of-concept study, *E.coli K12* was used as the model bacteria to test the system performance. A comparative study of immunoassays based on membranes and conventional 96-well plates was conducted. The contents are as follows: (1) The design and fabrication of the compact multichannel filtration device; (2) the minimization of background effects of membranes; (3) the assessment of *E.coli K12* collection and distribution on membranes; (4) the quantitative analysis of immunodetection results recorded with a smartphone camera.

## 2. Experimental section

### 2.1. Multichannel filtration device

The compact multichannel filtration device was manufactured using PlasCLEAR photoresist and a 3D printer (Asiga, Australia). The drawings were created using AutoCAD 2018 and then converted to the STL format for 3D printing. This filtration device consisted of the sampling head (Fig. 1a) and the main holder (Fig. 1b). In the sampling head, five holes with a diameter of 0.66 mm were assigned for the sampling needles. Correspondingly, another set of five holes with a 3 mm of diameter were configured as the filtrate channels in the main holder. To connect to the rubber cork of the suction flask, a funnel was incorporated at the bottom of the main holder (Fig. 1b). Four marks were added to ensure a good alignment of the sampling head and the main holder (Fig. 1a and b). Two

observation windows were included as well for inspecting the state of sample loading (Fig. 1b). The drawing of the assembled sampling head and the main holder as an integrated filtration device was shown as Fig. 1c.

### 2.2. Bacteria culture and counting

*E.coli K12* was used as the test bacteria. The liquid culture medium was prepared according to the Lysogeny Broth (LB) recipe for the amplification of seed *E.coli K12*. As for the solid culture medium, additional agar powder was added to achieve a concentration of 1.45% (w/w) in the prepared matrix. After the preparation, the mixed culture medium was stirred and then sterilized in the autoclave. The seed bacteria were inoculated into the liquid culture medium in a 50 ml centrifugal tube. Afterwards, the tube was placed in the incubator for 18 h at 37 °C. After the incubation, *E.coli K12* cells were centrifugally separated and then dispersed in the phosphate buffered saline (PBS) to prepare a stock sample. To quantify the concentration of *E.coli K12* cells, 100  $\mu$ l diluted stock sample (diluted  $10^5$  times in PBS buffer) was homogeneously coated onto the solid culture medium with a cell spreader. After the inoculation, the solid culture medium was incubated for 18 h at 37 °C. The *E.coli K12* concentration was quantified by enumerating the colonies on the incubated solid culture medium. Then the stock sample was diluted in PBS buffer to prepare the test samples with a series of varying concentrations for the immunodetection on membranes. The culture and enumeration of *B. subtilis* for the investigation of detection specificity were implemented according to the protocol as well. The concentrations of *E.coli K12* samples before and after the filtration via membranes with different pore sizes (0.2  $\mu$ m, 0.45  $\mu$ m and 0.8  $\mu$ m) were obtained through colony enumeration for the calculation of collection efficiency. The membranes were all pretreated with 0.1 N sodium hydroxide (NaOH) solution for 15 min. All operations including the extraction, inoculation, dispersion and dilution of *E.coli K12* cells were implemented on a clean bench.

### 2.3. Sample immobilization for SEM characterization

The specific procedures of immobilizing *E.coli K12* bacteria onto membranes for SEM (scanning electron microscopy) characterization were as follows. After filtration, the collected *E.coli K12* bacteria were fixed on membranes with a 2.5% (v/v) glutaraldehyde (G6257, Sigma) in the PBS buffer. Afterwards, the fixed samples were dehydrated in sequence by the ethanol with a series of concentrations (30%, 50%, 70%, 80%, and 100%). Each dehydration process lasted 10 min. After drying the samples, the membranes with immobilized *E.coli K12* cells

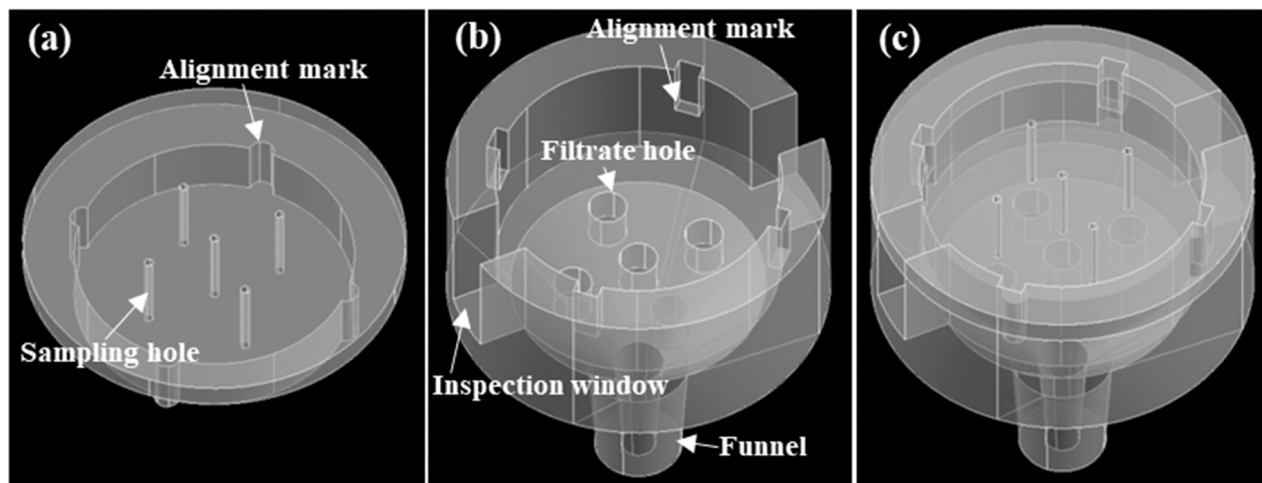


Fig. 1. The drawings of the compact filtration device. (a) The sampling head. (b) The main holder. (c) The assembled filtration device.

were sputtered with platinum (Pt) for SEM characterization.

#### 2.4. Immunodetection protocol

The primary antibody (ab137967, Abcam) and horseradish peroxidase (HRP) conjugated secondary antibody (ab205718, Abcam) were immediately made as aliquots using the 0.5 ml low-protein-adsorption centrifugal tubes after being received and stored at  $-20\text{ }^{\circ}\text{C}$  and  $4\text{ }^{\circ}\text{C}$ , respectively. Before use, the concentrations of the primary antibody and secondary antibody were diluted to  $0.2\text{ }\mu\text{g/ml}$  and  $0.5\text{ }\mu\text{g/ml}$  using 1% bovine serum albumin (BSA) added PBS buffer, respectively.

Cellulose acetate membrane was selected as the immunodetection substrate due to its low capacity of protein binding. Before loading *E. coli K12* samples, membranes with a 4 mm diameter were cut out using a hand-hold puncher from cellulose acetate membranes (C020A047A, 47 mm, VWR) and then were soaked in the 0.1 N NaOH solution for 15 min. After that pretreatment, the membranes were rinsed three times with purified water and then placed into the compact multichannel filtration device. The modification of membrane surface was characterized through the measurement of contact angle of water droplet using a high-speed camera. Subsequently, 5-ml *E. coli K12* test samples in PBS buffer with a series of prepared concentrations were loaded onto the membranes using a peristaltic pump within 30 min under a 0.1 MPa vacuum. Then  $20\text{ }\mu\text{l}$  of 2.5% BSA-PBS solution was added to each membrane for blocking the nonspecific binding sites. After 1 h of incubation, the membranes were rinsed twice using the 0.05% of Tween 20 loaded PBS buffer (PBST). As a surfactant, Tween 20 has been commonly used to effectively remove the excessive protein or antibody retained unexpectedly [22,25]. Afterwards, a drop of  $10\text{ }\mu\text{l}$  of primary antibody ( $0.2\text{ }\mu\text{g/ml}$ ) was added to each membrane (blank or sample loaded) and then was incubated for 1 h. After the washing with the PBST buffer for five times,  $10\text{ }\mu\text{l}$  HRP conjugated secondary antibody ( $0.5\text{ }\mu\text{g/ml}$ ) was added to each membrane followed with the incubation for another 1 h. After the washing with PBST buffer for five times,  $10\text{ }\mu\text{l}$  3, 3', 5, 5'-tetramethylbenzidine (TMB) substrate (34022, Thermo Fisher) was added to each membrane to trigger the color reaction. After 15 min,  $5\text{ }\mu\text{l}$  5% (v/v) sulfuric acid ( $\text{H}_2\text{SO}_4$ ) solution was added to each membrane to stop the reaction and stabilize the color. All developed colors on membranes were immediately recorded with a smartphone camera in a homemade photography box. All operations were implemented at room temperature. It should be noted that as the vacuum was shut off during the incubation, thus the reagent liquid could stay on membranes. After incubation or washing, all reagents and washing buffer were easily removed by the vacuum suction. The scheme of the immunodetection protocol on membranes was summarized in Fig. 2. The experiments for

comparing the background effects of membranes with and without surface modification were implemented with the same protocol after omitting the sample loading. It should be noted that despite the partial similarity of our assay to dot blot assays in general procedures and the volume of reagents required, our system has the advantage of continuous enrichment of micro targets [26].

For comparison, another commercial immunoassay protocol (provided by Abcam Company) using the same sample and reagents was employed for the immunodetection in 96-well plates.

#### 2.5. Quantification of immunodetection results

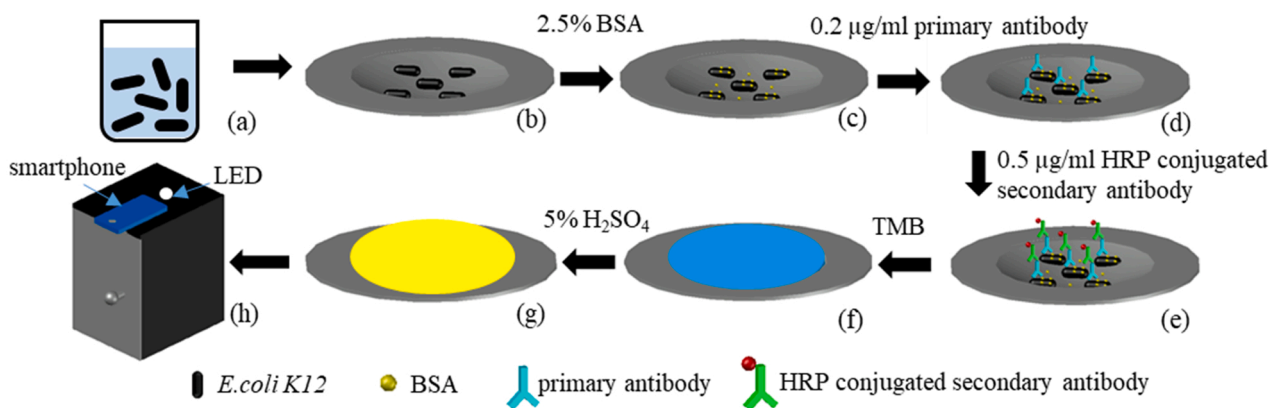
A homemade box was manufactured for photographing using a smartphone camera (shown in Fig. 2h). The distance between the LED and the membrane surface was set as 30 cm to achieve a uniform optical distribution. The optical uniformity was additionally tested and confirmed. A smartphone was placed at the window site of the photography box to record the developed color on the membranes. The developed color was then quantified using the ImageJ software based on the grayscale values of the red, green and blue color channels (RGB) [10]. The relative intensities of all color channels were acquired for interpreting the immunodetection results. The relative intensity was defined as the positive difference of the grayscale value of a specific color channel to the standard white color.

A white polydimethylsiloxane (PDMS, Sylgard 184, Dow Corning) pad was fabricated to hold the membranes for photography with a good contrast. It was placed on the main holder before loading the membranes. Calcium carbonate powder ( $\text{CaCO}_3$ , Sigma) was mixed with PDMS at a weight ratio of 3:10 to form a layer of matrix with a thickness of approximately 2 mm on abrasive paper to roughen the surface of PDMS and avoid optical reflection. After being degassed, the matrix was cured at  $70\text{ }^{\circ}\text{C}$  for 4 h. Afterwards, the white PDMS pad was peeled off from the abrasive paper, tailored as the required dimension and punched for five holes with a diameter of 0.6 mm.

### 3. Results and discussion

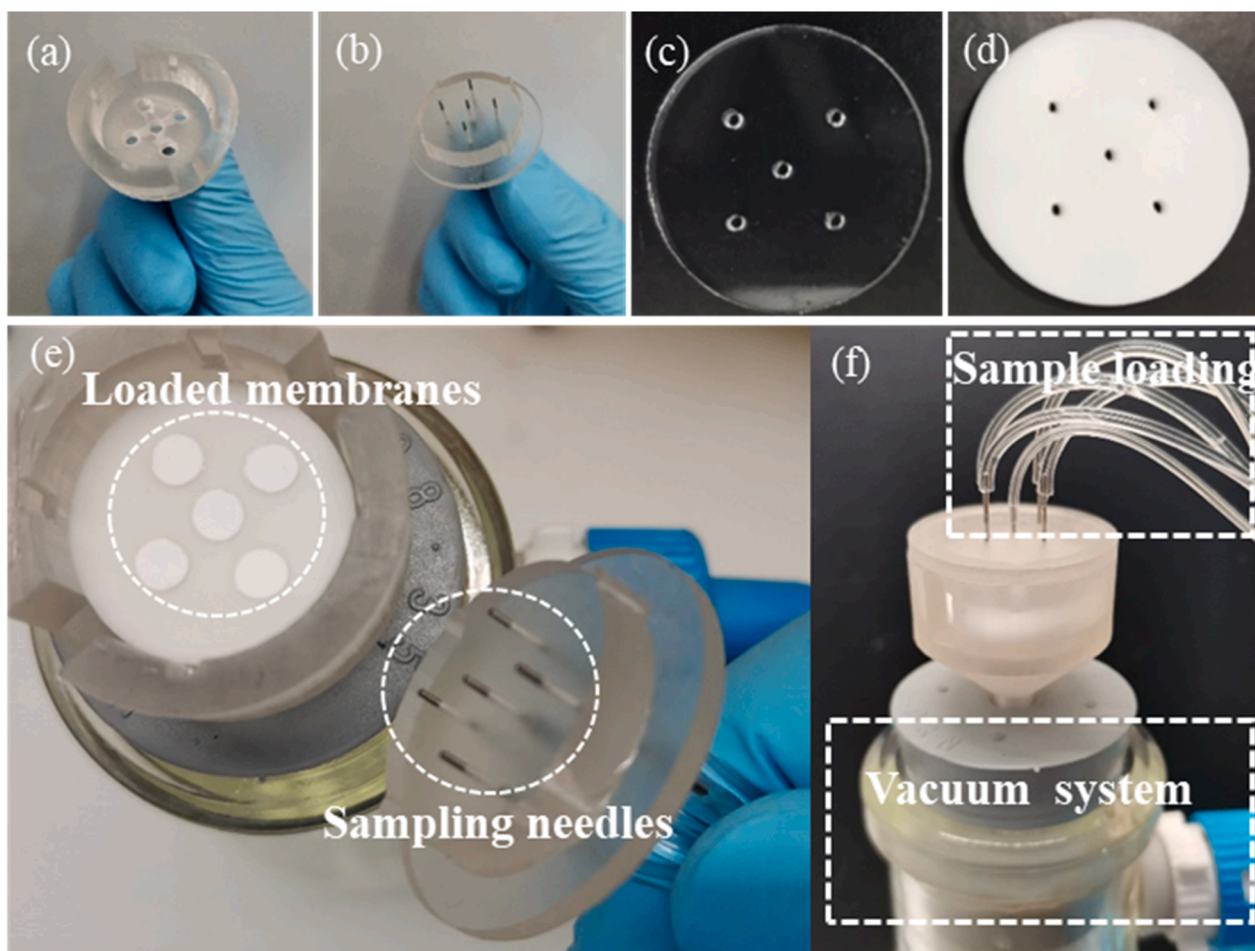
#### 3.1. 3D-printed compact multichannel filtration system

Fig. 3a and b showed the printed main holder and the sampling head, respectively. With the configuration of five channels, the analysis throughput was enhanced compared with that of single channel device. A comparison of the pure PDMS pad and the white PDMS pad was presented as Fig. 3c and d. As the pure PDMS surface was very smooth, the photograph had a poor quality due to the mirror reflection (Fig. 3c).



**Fig. 2.** Schematic of the membrane based immunoassay protocol. (a) Preparation of *E. coli K12* samples. (b) *E. coli K12* cells collected on the membranes. (c) Blocking the nonspecific protein binding sites. (d) Incubation of the primary antibody. (e) Incubation of the HRP conjugated secondary antibody. (f) Adding the TMB substrate to develop the color. (g) Adding the 5%  $\text{H}_2\text{SO}_4$  solution to stop the color reaction and to stabilize the color. (h) Recording the developed color using a smartphone camera in a homemade photography box.





**Fig. 3.** 3D printed filtration device, including (a) the main holder and (b) the sampling head. (c) The pure PDMS pad. (d) The white PDMS pad. (e) The loaded membranes and sampling needles. (f) The overview of the filtration device after being connected with the vacuum and sampling systems.

In contrast, no obvious mirror reflection was observed in Fig. 3d. Additionally, due to the addition of  $\text{CaCO}_3$  powder in the PDMS matrix, a white background was achieved with improved contrast for subsequent image analysis. Five pieces of cellulose acetate membranes (4 mm diameter) were loaded onto the white pad for collecting *E.coli K12* cells (Fig. 3e). As an approximately 1.6 mm of safety distance was set between membranes, no cross contamination was found during the sample loading and incubation. The membranes in this work were small and the consumed volume of antibody reagents for each sample was only 10  $\mu\text{l}$  while 100 and 500  $\mu\text{l}$  antibody reagents were generally needed for the immunoassays in 96-well-plate based assay and membrane based assay, respectively [21,22]. Fig. 3f showed the assembled filtration device after being connected to the suction flask and sampling systems.

### 3.2. Minimization of membrane background effects

The minimization of membrane background effects is of great importance for the interpretation of immunodetection results. Multiple reagents such as BSA, Western blocking reagent (WBR) and Tween-20 have been used to block the nonspecific binding sites of membranes to reduce the background effects [21,22,27]. However, their blocking performance could be attenuated after several cycles of buffer washing due to the weak interaction between the blocking molecules and the substrate. Here, as an alternative or in combination to blocking reagents, we have directly modified the membrane properties by pretreatment with 0.1 N NaOH solution before the immunodetection. The background effects of unmodified and modified cellulose acetate membranes were

compared as shown in Fig. 4a and b. After a sequence of operations by the protocol in Fig. 2, obvious yellow color developed on the unmodified cellulose acetate membrane. It suggested a substantial nonspecific adsorption of antibody molecules on the membranes despite a BSA blocking. In contrast, the membrane modified with the 0.1 N NaOH solution showed little color development, indicating the minimized background effect. The alkaline solutions have been used to oxidize the material surface for an increased material hydrophilicity [28,29]. It was assumed that the enhanced surface hydrophilicity could hinder the adsorption of protein molecules [30,31]. Considering the abundant ester groups of cellulose acetate (Fig. S1), a moderate hydrolysis might happen on the membrane surface in the alkaline environment. As a result, more hydroxyl groups were generated on the membrane surface, which substantially reduced the possibility of interaction between the antibody and the membrane material. This change was illustrated by the change of contact angle of water droplet on the surface of unmodified and modified membranes, as shown in Fig. 4c-f and g-j, respectively. The water droplet wetted the modified membrane surface immediately after contacting the surface while the wetting process proved much slower on the unmodified membrane surface. The initial contact angles were measured as 101.5 and 48.5 degree for unmodified and modified membranes, respectively. It should be noted that the cellulose acetate membrane could deteriorate after being immersed in the high concentration NaOH solution for a long time. According to Yamashita's investigation [32] and the experimental result in this study, the immersion of cellulose acetate membranes in 0.1 N NaOH solution for 15 min proved to be optimal for maintaining the membrane mechanical

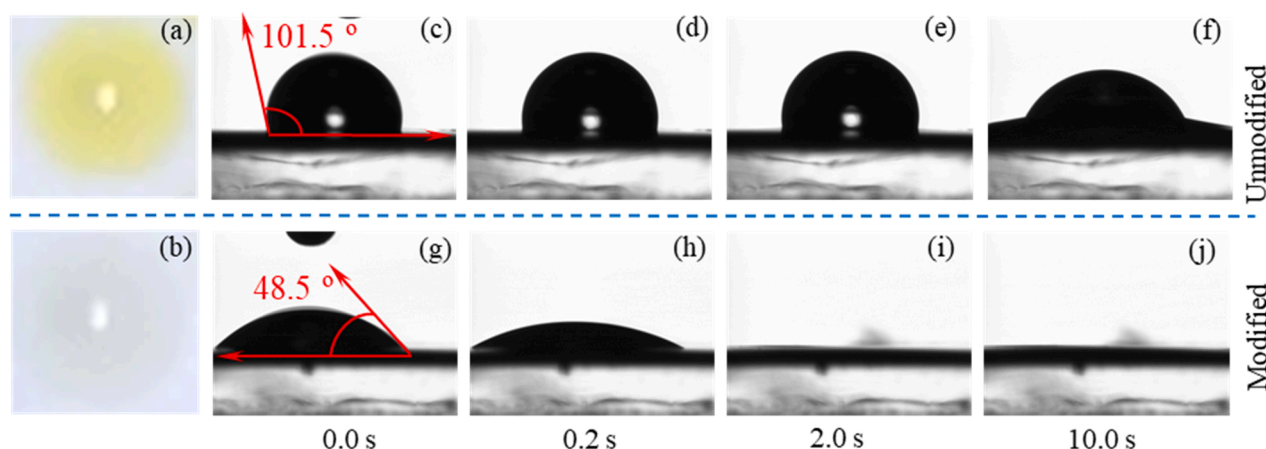


**Fig. 4.** Minimization of membrane background effects as seen on the smartphone picture of (a) the unmodified membrane and (b) the modified membrane after running a negative control experiment. (c-f) and (g-j) Time evolution of the contact angle of a water droplet on the unmodified and modified membrane surface, respectively. 0.00 s represented the time point of the droplet contacting the membrane surface.

strength and pore size.

### 3.3. Bacteria collected on membranes

*E.coli K12* cells could be collected by membranes with multiple mechanisms such as inertial impaction, physical interception and electrostatic interactions. To confirm the performance of membranes for collecting *E.coli K12* cells, the filtration efficiencies of cellulose acetate membranes with different pore sizes were compared. Fig. 5a indicated that *E.coli K12* cells could be completely collected by the membranes with a pore size of 0.45  $\mu\text{m}$  or 0.2  $\mu\text{m}$ . In contrast, approximately 15% of *E.coli K12* bacteria penetrated through the membranes with a 0.8  $\mu\text{m}$  pore size. In this study, considering the typical size of *E.coli K12* bacteria within 0.5–2  $\mu\text{m}$ , membranes with a 0.45  $\mu\text{m}$  pore size were used as the substrate for the integrated sample enrichment and immunodetection. Fig. 5b and c respectively presented the distribution of *E.coli K12* with different densities on cellulose acetate membranes (0.2 cfu/100  $\mu\text{m}^2$  and 20 cfu/100  $\mu\text{m}^2$ ). Due to the confined filtration area on the miniaturized membranes, a higher surface density of *E.coli K12* could be achieved leading to a more sensitive development of signal color, compared with that of large membranes.

### 3.4. Immunodetection results

The optical homogeneity for photographing the immunodetection

results was investigated using the white PDMS pad. The variance coefficients of the relative intensity of the three color channels among different sites on the white PDMS pad were all smaller than 0.27% (Fig. S2), implying a homogeneous optical distribution. As shown in Fig. 6a, various levels of color brightness were developed on the membranes as a result of immunodetection. Since the detection specificity is mainly dependent on the specificity of the primary antibody used if the matrix interference is negligible, such a configuration of multiple detection channels makes it possible to detect multiple bacteria as well in parallel using the corresponding specific primary antibodies. In Fig. 6b, the relative intensities of the three color channels were all extracted for a comparative study. The reproducibility was good according to the repeated experiments with an average coefficient of variation 3.7–7.8% for all the three colors. It was found that the blue channel was most sensitive to the change of *E.coli K12* concentration especially when the concentration was higher than 400 cfu/ml. However, the blue color could not differentiate the 400 cfu/ml sample from the blank samples according to the threshold. The signal threshold was conventionally defined as three times the noise level plus the blank level. The noise level was assumed as the standard deviation of the relative intensity for blank samples. In contrast, as the relative intensity was higher than the signal threshold ( $T$ -test,  $p = 0.0013$ ), the 400 cfu/ml samples could be well identified using the red channel despite a low overall sensitivity (Fig. 6c). The performance difference of element colors suggested a combined strategy for the interpretation of

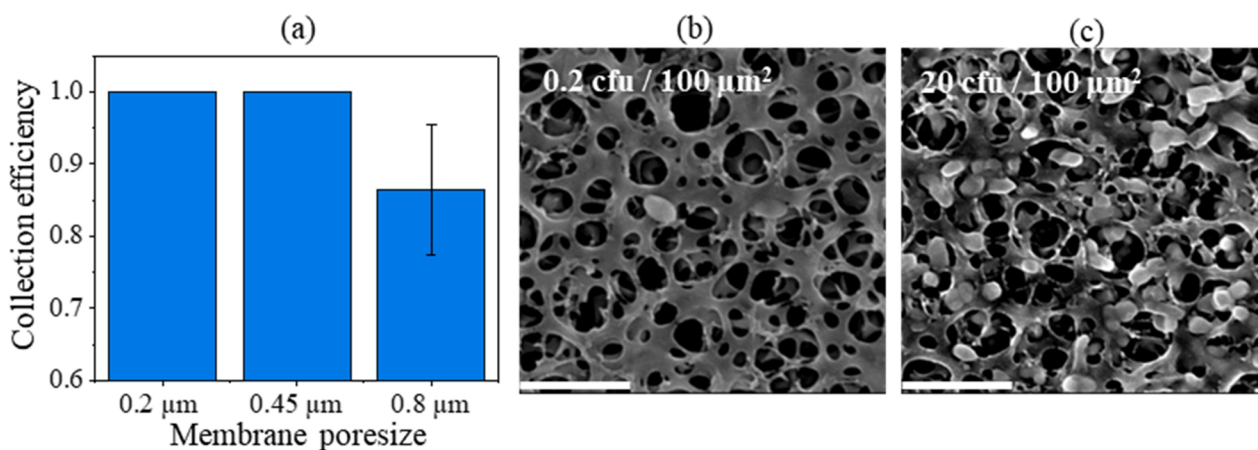


**Fig. 5.** The collection of *E.coli K12* cells. (a) Comparison of the collection efficiency of cellulose acetate membranes with different pore sizes. SEM images indicating different densities of *E. coli K12* cells on membranes, (b) 0.2 cfu/100  $\mu\text{m}^2$ . (c) 20 cfu/100  $\mu\text{m}^2$ . Scale bar in images: 5  $\mu\text{m}$ .

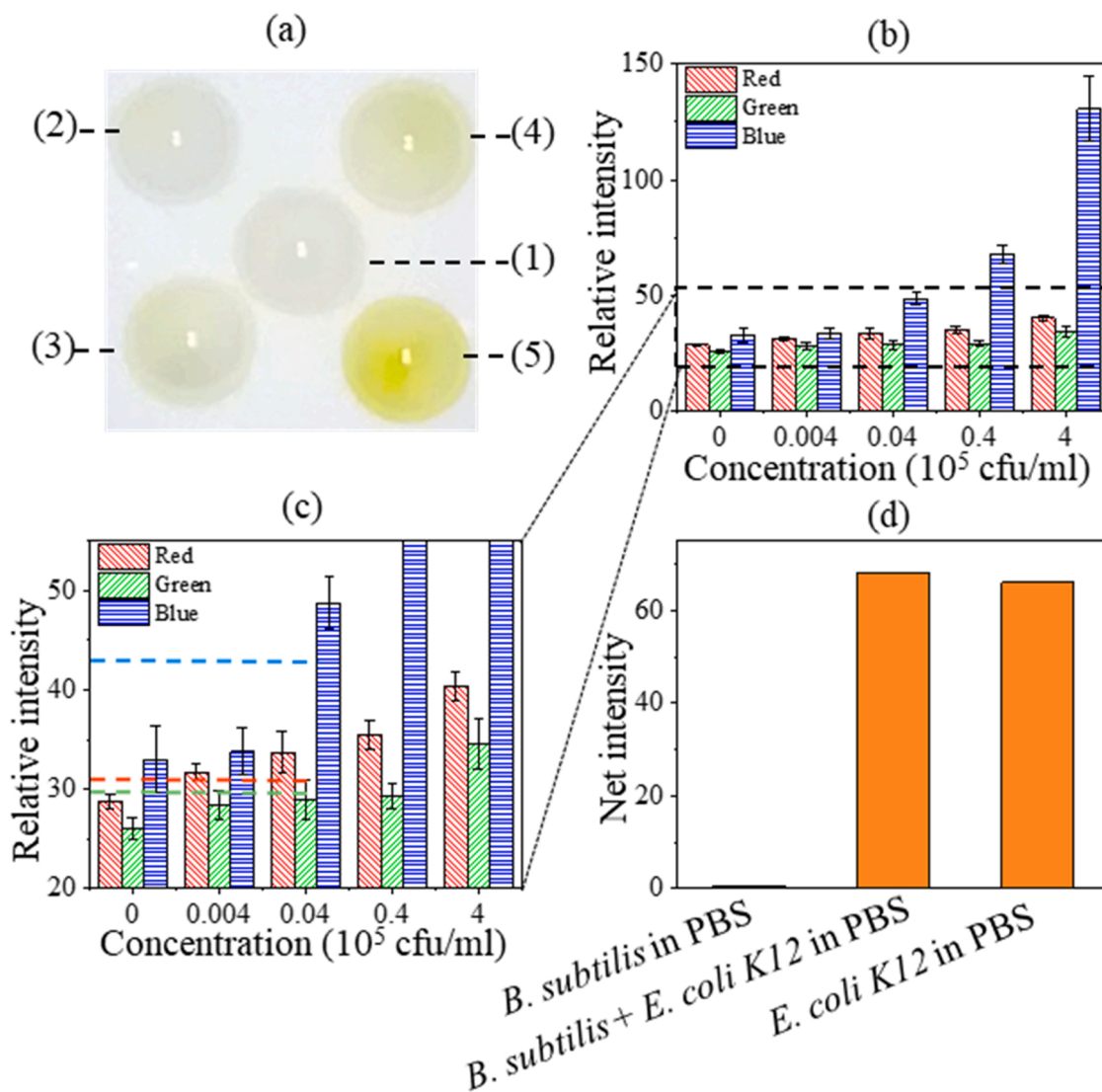


**Fig. 6.** Immunodetection results. (a) Picture of the developed signal on the membrane for (1) blank samples, (2)  $0.004 \times 10^5$  cfu/ml, (3)  $0.04 \times 10^5$  cfu/ml, (4)  $0.4 \times 10^5$  cfu/ml, (5)  $4 \times 10^5$  cfu/ml. (b) Quantification of immunodetection results with the RGB interpretation. (c) The magnified part of Fig. 6c. The signal thresholds for red, green and blue elements were respectively marked with red, green and blue dash lines in Fig. 6c. (d) The results corresponding to  $0.6 \times 10^5$  cfu/ml *B. subtilis* in PBS, the mixture of  $0.6 \times 10^5$  cfu/ml *B. subtilis* and  $2 \times 10^5$  cfu/ml *E. coli* K12 in PBS and  $2 \times 10^5$  cfu/ml *E. coli* K12 in PBS.

immunodetection results instead of merely considering a single element color. For a comparative study, the immunodetection results in 96-well plates with a limit of detection about  $10^4$ - $10^5$  cfu/ml were presented in Fig. S3. 400 cfu/ml of *E. coli* K12 was detectable using the membrane-based immunoassay and the limit of detection was calculated as 40 cfu/ml according to the regression relationship between the relative intensity of red color and the concentration of *E. coli* K12, representing a significant improvement compared to the result from 96-well plates and other low-cost colorimetric assays [18–20]. Compared results were summarized in Table S1. Although a lower detection limit was achieved in other researchers' studies based on advanced instruments such as absorbance reader, fluorescence microscopy and spectrometer [9,22, 23], our work provided a low-cost and simple solution for the immunodetection of pathogens with little dependence on analysis instruments. The specificity of detecting *E. coli* K12 was investigated using *B. subtilis* in PBS buffer and real river water. The net intensity represented the positive difference of relative intensity corresponding to the blue color between the test sample and blank sample. The signal response to *B. subtilis* ( $0.6 \times 10^5$  cfu/ml in PBS) was small and no significant signal differences could be observed when comparing the

mixture of *B. subtilis* and *E. coli* K12 ( $0.6 \times 10^5$  cfu/ml and  $2 \times 10^5$  cfu/ml in PBS) and *E. coli* K12 alone ( $2 \times 10^5$  cfu/ml in PBS), as shown in Fig. 6d. It demonstrated negligible interferences of *B. subtilis* on the immunodetection of *E. coli* K12. However, nonspecific signals appeared in the test of real river water (Limmat river in Zurich), as shown in Fig. S4, showing significant interferences from complex environmental matrix. The composition in river water is usually complicated, including ions, organic matter, biological substances, microelements, etc. [33] These interferences may originate the non-specific binding of antibody on aquatic species intercepted on membranes. Additionally, the primary antibody used in the protocol is a polyclonal one, which may lower the specificity of immunodetection as well in real matrices.

#### 4. Conclusions

In this study, a compact filtration device with five channels was manufactured for the colorimetric immunodetection with integrated sample enrichment on a cellulose acetate membrane. *E. coli* K12 cells could be collected with 100% efficiency on membranes with a  $0.45 \mu\text{m}$  pore size. Background effects of membranes were successfully



minimized through the pretreatment using the 0.1 N sodium hydroxide solution. Quantitative analysis was achieved using a smartphone camera and RGB data analysis, enabling the detection of 400 cfu/ml *E.coli K12*, two orders of magnitude more sensitive with that of 96-well plates based assays. Thanks to the little dependence on advanced analysis instruments, significantly reduced reagents consumption and multiple channels in a compact filtration device, this study provided a low-cost and simple solution for the immunodetection of pathogens with improved throughput and detection limit. For the future work, more efforts are needed to optimize the protocol to analyze real environmental and food samples. Additionally, it will be necessary to implement all the procedures of immunoassay in an automated fashion.

#### CRedit authorship contribution statement

J.T. conceived of the idea, implemented all the experiments and wrote the manuscript. Y.M. fabricated the compact filtration system. L. B. did the measurement of contact angle on membrane surface. G.Q. assisted to establish the optical system. Y.Y. provided the guidance in bacteria culture and enumeration. X.Z. provided the guidance in data interpretation. All co-authors provided comments. J.W. supervised this work.

#### Declaration of Competing Interest

The authors declare no conflicts of interest.

#### Acknowledgments

This work was partially supported by Center for Filtration Research at University of Minnesota, USA (Subaward No. W530672710).

#### Appendix A. Supporting information

Supplementary data associated with this article can be found in the online version at [doi:10.1016/j.snb.2021.131142](https://doi.org/10.1016/j.snb.2021.131142).

#### References

- [1] F.Y. Ramírez-Castillo, A. Loera-Muro, M. Jacques, P. Garneau, F.J. Avelar-González, J. Harel, A.L. Guerrero-Barrera, Waterborne pathogens: detection methods and challenges, *Pathogens* 4 (2) (2015) 307–334.
- [2] J.T. Connelly, A.J. Baeumner, Biosensors for the detection of waterborne pathogens, *Anal. Bioanal. Chem.* 402 (1) (2012) 117–127.
- [3] H. Bridle, B. Miller, M.P.Y. Desmulliez, Application of microfluidics in waterborne pathogen monitoring: a review, *Water Res.* 55 (2014) 256–271.
- [4] Q. Liu, X. Zhang, Y. Yao, W. Jing, S. Liu, G. Sui, A novel microfluidic module for rapid detection of airborne and waterborne pathogens, *Sens. Actuators B Chem.* 258 (2018) 1138–1145.
- [5] Q. Liu, Y. Zhang, W. Jing, S. Liu, D. Zhang, G. Sui, First airborne pathogen direct analysis system, *Analyst* 141 (5) (2016) 1637–1640.
- [6] C.F. Fronczek, J.-Y. Yoon, Biosensors for monitoring airborne pathogens, *J. Lab. Autom.* 20 (4) (2015) 390–410.
- [7] L. Zheng, G. Cai, S. Wang, M. Liao, Y. Li, J. Lin, A microfluidic colorimetric biosensor for rapid detection of *Escherichia coli* O157:H7 using gold nanoparticle aggregation and smart phone imaging, *Biosens. Bioelectron.* 124–125 (2019) 143–149.
- [8] S. Chattopadhyay, A. Kaur, S. Jain, H. Singh, Sensitive detection of food-borne pathogen *Salmonella* by modified PAN fibers-immunoassay, *Biosens. Bioelectron.* 45 (2013) 274–280.
- [9] L. Xue, F. Huang, L. Hao, G. Cai, L. Zheng, Y. Li, J. Lin, A sensitive immunoassay for simultaneous detection of foodborne pathogens using MnO<sub>2</sub> nanoflowers-assisted loading and release of quantum dots, *Food Chem.* 322 (2020), 126719.
- [10] K. Mahato, P. Chandra, Paper-based miniaturized immunosensor for naked eye ALP detection based on digital image colorimetry integrated with smartphone, *Biosens. Bioelectron.* 128 (2019) 9–16.
- [11] O. Lazcka, F.J.D. Campo, F.X. Muñoz, Pathogen detection: A perspective of traditional methods and biosensors, *Biosens. Bioelectron.* 22 (7) (2007) 1205–1217.
- [12] J.A. Adkins, K. Boehle, C. Friend, B. Chamberlain, B. Bisha, C.S. Henry, Colorimetric and electrochemical bacteria detection using printed paper- and transparency-based analytic devices, *Anal. Chem.* 89 (6) (2017) 3613–3621.
- [13] G. Qiu, Y. Yue, J. Tang, Y.-B. Zhao, J. Wang, Total bioaerosol detection by a succinimidyl-ester-functionalized plasmonic biosensor to reveal different characteristics at three locations in Switzerland, *Environ. Sci. Technol.* 54 (3) (2020) 1353–1362.
- [14] J.D. Oliver, Recent findings on the viable but nonculturable state in pathogenic bacteria, *FEMS Microbiol. Rev.* 34 (4) (2010) 415–425.
- [15] R. Wang, K. Kim, N. Choi, X. Wang, J. Lee, J.H. Jeon, G.-E. Rhie, J. Choo, Highly sensitive detection of high-risk bacterial pathogens using SERS-based lateral flow assay strips, *Sens. Actuators B Chem.* 270 (2018) 72–79.
- [16] P. Chen, M. Gates-Hollingsworth, S. Pandit, A. Park, D. Montgomery, D. AuCoin, J. Gu, F. Zenhausern, Paper-based Vertical Flow Immunoassay (VFI) for detection of bio-threat pathogens, *Talanta* 191 (2019) 81–88.
- [17] G.A. Posthuma-Trumpie, J. Korf, A. van Amerongen, Lateral flow (immuno)assay: its strengths, weaknesses, opportunities and threats. A literature survey, *Anal. Bioanal. Chem.* 393 (2) (2009) 569–582.
- [18] E. Eltzov, R.S. Marks, Miniaturized flow stacked immunoassay for detecting *Escherichia coli* in a single step, *Anal. Chem.* 88 (12) (2016) 6441–6449.
- [19] C. Song, C. Liu, S. Wu, H. Li, H. Guo, B. Yang, S. Qiu, J. Li, L. Liu, H. Zeng, X. Zhai, Q. Liu, Development of a lateral flow colloidal gold immunoassay strip for the simultaneous detection of *Shigella boydii* and *Escherichia coli* O157:H7 in bread, milk and jelly samples, *Food Control* 59 (2016) 345–351.
- [20] C. Song, J. Liu, J. Li, Q. Liu, Dual FITC lateral flow immunoassay for sensitive detection of *Escherichia coli* O157:H7 in food samples, *Biosens. Bioelectron.* 85 (2016) 734–739.
- [21] N. Párraga-Niño, S. Quero, A. Ventós-Alfonso, N. Uria, O. Castillo-Fernandez, J. J. Ezenarro, F.-X. Muñoz, M. García-Nuñez, M. Sabrià, New system for the detection of *Legionella pneumophila* in water samples, *Talanta* 189 (2018) 324–331.
- [22] J.J. Ezenarro, N. Uria, Ó. Castillo-Fernández, N. Párraga, M. Sabrià, F.X. Muñoz Pascual, Development of an integrated method of concentration and immunodetection of bacteria, *Anal. Bioanal. Chem.* 410 (1) (2018) 105–113.
- [23] X. Lin, X. Huang, Y. Zhu, K. Urmann, X. Xie, M.R. Hoffmann, Asymmetric membrane for digital detection of single bacteria in milliliters of complex water samples, *ACS Nano* 12 (10) (2018) 10281–10290.
- [24] S. Schwaminger, M.E. Rottmueller, R. Fischl, B. Kalali, S. Berensmeier, Detection of targeted bacteria species on filtration membranes, *Analyst* 146 (11) (2021) 3549–3556.
- [25] T. Waritani, J. Chang, B. McKinney, K. Terato, An ELISA protocol to improve the accuracy and reliability of serological antibody assays, *MethodsX* 4 (2017) 153–165.
- [26] L. Li, Z. Liu, H. Zhang, W. Yue, C.-W. Li, C. Yi, A point-of-need enzyme linked aptamer assay for *Mycobacterium tuberculosis* detection using a smartphone, *Sens. Actuators B Chem.* 254 (2018) 337–346.
- [27] D. Huber, J. Rudolf, P. Ansari, B. Galler, M.; Führer, C.; Hasenhindl, S. Baumgartner, Effectiveness of natural and synthetic blocking reagents and their application for detecting food allergens in enzyme-linked immunosorbent assays, *Anal. Bioanal. Chem.* 394 (2) (2009) 539–548.
- [28] Y. Mao, Q. Zhao, T. Pan, J. Shi, S. Jiang, M. Chen, B. Zhou, Y. Tian, Platinum porphyrin/3-(trimethoxysilyl)propylmethacrylate functionalized flexible PDMS micropillar arrays as optical oxygen sensors, *N. J. Chem.* 41 (13) (2017) 5429–5435.
- [29] S.K. Vashist, E.M. Schneider, J.H.T. Luong, Surface plasmon resonance-based immunoassay for human fetuin A, *Analyst* 139 (9) (2014) 2237–2242.
- [30] M. Rabe, D. Verdes, S. Seeger, Understanding protein adsorption phenomena at solid surfaces, *Adv. Colloid Interface Sci.* 162 (1) (2011) 87–106.
- [31] K. Wang, C. Zhou, Y. Hong, X. Zhang, A review of protein adsorption on bioceramics, *Interface Focus* 2 (3) (2012) 259–277.
- [32] Y. Yamashita, T. Endo, Deterioration behavior of cellulose acetate films in acidic or basic aqueous solutions, *J. Appl. Polym. Sci.* 91 (5) (2004) 3354–3361.
- [33] A. Nikanorov, L. Brazhnikova, Water chemical composition of rivers, lakes and wetlands, *Types Prop. Water* 2 (2009) 42–80.

**Jiukai Tang** is currently a Ph.D. candidate under the direction of Prof. Jing Wang at the Institute of Environmental Engineering, ETH Zürich. His research interests include optofluidics, analytical chemistry, and biosensors.

**Yingchao Meng** is a PhD student at the Institute of Chemical and Bioengineering, ETH Zürich. His main research interest is the development of microfluidic platforms for extracellular vesicle separation and rare cell enrichment.

**Léonard Bezingue** started his PhD studies in 2019 under the supervision of Prof. Shih and Prof. deMello at the Institute of Chemical and Bioengineering, ETH Zürich. His current research interests focus on the development of paper-based electrochemical biosensors for rapid diagnostic testing.

**Guangyu Qiu** is a postdoctoral Researcher at ETH Zurich. He obtained his Ph.D. from City University of Hong Kong. His research area includes applied optics and plasmonics, functional materials in nano-optics, chemical, biochemical and environmental sensing applications.

**Yang Yue** is a Postdoc at the Institute of Environmental Engineering, ETH Zürich. His main research interests include environmental toxicity and bioaerosol analysis.

**Xiaole Zhang** is a Postdoc at the Institute of Environmental Engineering, ETH Zürich. His main research interests include aerosol transmission and health effects.



**Jing Wang** is an associate professor at the Institute of Environmental Engineering, ETH Zürich. His main research interests include air pollution control, nanoparticle transport

and emission reduction, instrumentation for airborne nanoparticle measurement, developing sensors using electrochemical and optical methods.